

CPP-95-11

DOE-ER40757-068

NUHEP-TH-95-07

July 1995

Strange-Beauty Meson Production at $p\bar{p}$ Colliders

Kingman Cheung*

Center for Particle Physics, University of Texas, Austin, TX 78712

Robert J. Oakes†

Department of Physics and Astronomy, Northwestern University, Evanston, IL 60208

Abstract

The production rates and transverse momentum distributions of the strange-beauty mesons B_s and B_s^* at $p\bar{p}$ colliders are calculated assuming fragmentation is the dominant process. Results are given for the Tevatron in the large transverse momentum region, where fragmentation is expected to be most important.

I. INTRODUCTION

Data on the production of strange B mesons is rapidly accumulating. At LEP the DELPHI Collaboration has measured the probability for a \bar{b} antiquark to hadronize into a weakly

*Internet address: cheung@utpapa.ph.utexas.edu

†Internet address: oakes@fnalv.fnal.gov

decaying strange B meson [1]. Assuming the hadronization is dominated by the fragmentation of the heavy \bar{b} antiquark, we determined the fragmentation functions $D_{\bar{b} \rightarrow B_s}(z, \mu)$ and $D_{\bar{b} \rightarrow B_s^*}(z, \mu)$ from the measured total probability for a \bar{b} antiquark to hadronize into the lowest strange-beauty states $B_s(^1S_0)$ and $B_s^*(^3S_1)$ [2]. Here z is the fraction of the \bar{b} antiquark momentum carried by the B_s or B_s^* at the scale μ . The momentum distributions of the B_s and B_s^* mesons produced in e^+e^- annihilation at the energy of the Z mass were then predicted [2].

Here we extend our calculations to the production of the B_s and B_s^* states in $p\bar{p}$ annihilation at the Tevatron, using the fragmentation functions previously determined from the e^+e^- data taken at LEP. Sec. II presents the cross section for the process in terms of the parton distribution functions and subprocesses and the fragmentation functions, which we discuss in Secs. III and IV, respectively. In Sec. V we present numerical results for the transverse momentum (p_T) distributions of the strange B_s and B_s^* mesons, as well as the total cross section for $p_T > p_T^{\min}$. Finally, we discuss these results and summarize our conclusions.

II. CROSS SECTIONS

In the parton model the cross section for the production by fragmentation of strange B mesons in proton-antiproton annihilation involves three main factors: the structure functions of the initial partons in the proton and antiproton, the subprocess in which the initial partons produce a particular parton in the final state, and the fragmentation of this final parton into the strange B meson. The transverse momentum distribution of the B_s meson is then of the form

$$\frac{d\sigma}{dp_T} = \sum_{i,j,k} \int dx_i \int dx_j \int dz f_{i/p}(x_i) f_{j/\bar{p}}(x_j) \frac{d\hat{\sigma}}{dp_T} \left(i(x_i) j(x_j) \rightarrow k\left(\frac{p_T}{z}\right) X; \mu \right) D_{k \rightarrow B_s}(z; \mu) . \quad (1)$$

Here $f_{i/p}(x_i)$ and $f_{j/\bar{p}}(x_j)$ are the structure functions of the initial partons i and j carrying fractions of the total momenta x_i and x_j in the proton and antiproton, respectively. The

production of parton k with momentum p_T/z is described by the hard subprocess cross section $\hat{\sigma}$ at the scale μ . And $D_{k \rightarrow B_s}(z; \mu)$ is the fragmentation function for the parton k to yield the meson B_s with momentum fraction z at the scale μ . The factorization scale μ is of the order of the transverse momentum of the fragmenting parton. The soft physics is contained in the structure functions, while the parton subprocess is a hard process and can be reliably calculated in perturbation theory. We shall also assume the fragmentation of \bar{b} into B_s is also a hard process, an assumption that will require further discussion below, since the s quark is not very heavy.

Clearly, there is a formula very similar to Eq. (1) for the production of the B_s^* , which we need not write explicitly. Because the radiative decay $B_s^* \rightarrow B_s + \gamma$ is so fast and the $B_s^* - B_s$ mass difference is so small, the transverse momentum of B_s^* is hardly affected in the decay $B_s^* \rightarrow B_s + \gamma$, and thus contributes to the inclusive production of the B_s . We will, therefore, present each individually in the figures showing $d\sigma/dp_T$ and $\sigma(p_T > p_T^{\min})$ and also include their sum in a table, for convenience.

In the fragmentation process $k \rightarrow B_s$ we have included gluons as well as \bar{b} antiquarks. Although the direct $g \rightarrow B_s$ fragmentation process does not occur until order α_s^3 there is a significant contribution coming from the Altarelli-Parisi evolution of the \bar{b} antiquark fragmentation functions from the heavy quark mass to the collider energy scale Q , which is of order $\alpha_s^3 \log(Q/m_b)$ due to the splitting $g \rightarrow \bar{b}$. This has been shown to be significant for the production of B_c mesons [3] and we have also included it here.

III. STRUCTURE FUNCTIONS AND PARTON SUBPROCESSES

In Eq. (1) we have assumed a factorization scale μ , with the parton distribution functions being due to soft processes below this scale, while the parton cross sections for the subprocesses are due to hard contributions above this scale. For the parton distribution functions we used the most recent CTEQ version 3 [4], in which we chose the leading-order fit, since our calculation is also a leading-order one. For the subprocesses we used the tree-

level cross sections, to be consistent, since the parton fragmentation functions, which are discussed in the following section, were calculated only to leading order. For the production of \bar{b} antiquarks we included the processes $gg \rightarrow b\bar{b}$, $g\bar{b} \rightarrow g\bar{b}$, and $q\bar{q} \rightarrow b\bar{b}$, while for the production of gluons g we included the processes $gg \rightarrow gg$, $gq(\bar{q}) \rightarrow gq(\bar{q})$, and $q\bar{q} \rightarrow gg$, where q denotes any of the quarks, u, d, s, c, b .

For the running strong coupling constant α_s we used the simple one-loop result evolved from its value at $\mu = m_Z$:

$$\alpha_s(\mu) = \frac{\alpha_s(m_Z)}{1 + \frac{33-2n_f}{6\pi} \alpha_s(m_Z) \log\left(\frac{\mu}{m_Z}\right)}. \quad (2)$$

Here n_f is the number of active flavors at the scale μ and we chose $\alpha_s(m_Z) = 0.117$ [5]. From the experimental results on b -quark production cross sections at the Tevatron we know that there are discrepancies between the calculations and the experiments about a factor of two. Therefore, adopting a more complicated form for the strong coupling constant, or using the next-to-leading order subprocess cross sections, or taking the next-to-leading order structure functions is not critical. At this point, we are primarily interested in how important the fragmentation process is for B_s and B_s^* production and how the shapes of the calculated momentum distributions compare with forthcoming data.

The factorization scale μ in Eq. (1) deserves further discussion before proceeding. The scale μ superficially appears to have been invented only to separate the production of B_s mesons into structure functions, subprocess cross sections, and fragmentation functions. In principle, this is so and the production is independent of the choice of μ . But in practice, the results do depend on μ , since only if all the factors are calculated to all orders in α_s will the dependence on μ cancel. However, for example, the fragmentation functions were calculated only to leading order and, consequently, the results will depend on μ . We shall investigate the sensitivity of the results to the choice of μ by varying μ from $\mu_R/2$ to $2\mu_R$, where $\mu_R = \sqrt{p_T^2(\text{parton}) + m_b^2}$ is our central choice of the scale μ .

IV. FRAGMENTATION FUNCTIONS

To obtain the fragmentation functions at the scale μ we have numerically integrated the Altarelli-Parisi evolution equations [6] from the scale μ_0 , which is of the order of the b -quark mass. The evolution equations for the fragmentation functions $D_{\bar{b} \rightarrow B_s}(z, \mu)$ and $D_{g \rightarrow B_s}(z, \mu)$ are

$$\mu \frac{\partial}{\partial \mu} D_{\bar{b} \rightarrow B_s}(z, \mu) = \int_z^1 \frac{dy}{y} P_{\bar{b} \rightarrow \bar{b}}(z/y, \mu) D_{\bar{b} \rightarrow B_s}(y, \mu) + \int_z^1 \frac{dy}{y} P_{\bar{b} \rightarrow g}(z/y, \mu) D_{g \rightarrow B_s}(y, \mu), \quad (3)$$

and

$$\mu \frac{\partial}{\partial \mu} D_{g \rightarrow B_s}(z, \mu) = \int_z^1 \frac{dy}{y} P_{g \rightarrow \bar{b}}(z/y, \mu) D_{\bar{b} \rightarrow B_s}(y, \mu) + \int_z^1 \frac{dy}{y} P_{g \rightarrow g}(z/y, \mu) D_{g \rightarrow B_s}(y, \mu), \quad (4)$$

with similar, coupled equations for the B_s^* fragmentation functions. The splitting functions $P_{i \rightarrow j}(x, \mu)$, to leading order in $\alpha_s(\mu)$, are explicitly given in Ref. [3]. As boundary conditions in these calculations we have used the fragmentation functions at the scale μ_0 calculated in Ref. [7]:

$$\begin{aligned} D_{\bar{b} \rightarrow B_s}(z, \mu_0) &= \frac{2\alpha_s(2m_s)^2 |R(0)|^2}{81\pi m_s^3} \frac{rz(1-z)^2}{(1-(1-r)z)^6} \\ &\times [6 - 18(1-2r)z + (21 - 74r + 68r^2)z^2 \\ &\quad - 2(1-r)(6 - 19r + 18r^2)z^3 + 3(1-r)^2(1-2r+2r^2)z^4]. \end{aligned} \quad (5)$$

Here z is the fraction of the \bar{b} antiquark momentum carried by the B_s meson, $r = m_s/(m_b + m_s)$, and $R(0)$ is the B_s meson S -wave radial wavefunction at the origin. The corresponding fragmentation function for $\bar{b} \rightarrow B_s^*$ is [7]

$$\begin{aligned} D_{\bar{b} \rightarrow B_s^*}(z, \mu_0) &= \frac{2\alpha_s(2m_s)^2 |R(0)|^2}{27\pi m_s^3} \frac{rz(1-z)^2}{(1-(1-r)z)^6} \\ &\times [2 - 2(3-2r)z + 3(3-2r+4r^2)z^2 \\ &\quad - 2(1-r)(4-r+2r^2)z^3 + (1-r)^2(3-2r+2r^2)z^4], \end{aligned} \quad (6)$$

The induced gluon fragmentation functions $D_{g \rightarrow B_s, B_s^*}(z, \mu)$ are of order $\alpha_s^3 \log(\mu/m_b)$ and become important at large values of the scale μ relative to the \bar{b} antiquark fragmentation

functions $D_{\bar{b} \rightarrow B_s, B_s^*}(z, \mu)$, which are of order $\alpha_s^2(\mu)$. The boundary conditions for the gluon fragmentation functions are

$$D_{g \rightarrow B_s}(z, \mu) = D_{g \rightarrow B_s^*}(z, \mu) = 0 \quad (7)$$

for $\mu \leq 2(m_b + m_s)$, the threshold for producing B_s or B_s^* mesons from a gluon.

The value of $|R(0)|^2$ can be determined from the decay constant f_{B_s} of the B_s meson using the relation [8]

$$f_{B_s}^2 = \frac{3}{\pi} \frac{|R(0)|^2}{M_{B_s}} \quad (8)$$

with $f_{B_s} = 207 \pm 34 \pm 22$ MeV [9] and $M_{B_s} = 5.375$ GeV [5].

If we choose the b quark mass to be $m_b = 5$ GeV the only remaining parameter in these fragmentation functions is m_s . This strange-quark mass parameter m_s has been determined previously [2] using the same initial fragmentation functions from the experimental value [1] of the probability f_s^w for a \bar{b} antiquark to fragment into weakly decaying strange-beauty mesons:

$$f_s^w = \int_0^1 dz \left[D_{\bar{b} \rightarrow B_s}(z, \mu_0) + D_{\bar{b} \rightarrow B_s^*}(z, \mu_0) \right] . \quad (9)$$

Since the total probability for the \bar{b} antiquark to fragment into a B meson is independent of scale, the initial scale μ_0 in Eq. (9), which is of the order of the b -quark mass, was chosen to be $\mu_0 = m_b + 2m_s$ as in Ref. [7]. We previously found [2] $m_s = 318^{+47}_{-24}$ MeV/ c^2 based on the DELPHI measurement $f_s^w = 0.19 \pm 0.06 \pm 0.08$ and assuming $\alpha_s(m_Z) = 0.12$. Prior to the DELPHI measurement there were older data from LEP [10] which were consistent with this measurement. There is now also a new measurement from CDF [11] of the quantity

$$\frac{\sigma(B_s)}{\sigma(B_u) + \sigma(B_d)} = 0.26^{+.17}_{-.08} \pm .08 . \quad (10)$$

Since the total fragmentation probability $P(b \rightarrow \text{baryon}) \approx 5-10\%$, the corresponding value of $f_s^w = P(\bar{b} \rightarrow B_s, B_s^*)$ can be estimated assuming $P(\bar{b} \rightarrow B_u + B_d + B_s + \text{baryons}) = 1$. Using the newer CDF data, Eq. (10), we obtain $f_s^w = 0.196(0.186)$ for $P(\bar{b} \rightarrow \text{baryon}) = 5(10)\%$,

which is consistent with the DELPHI measurement. In the present calculations, therefore, we used the same value $f_s^w = 0.19 \pm 0.06 \pm 0.08$ [1] but a slightly different value of $\alpha_s(m_Z) = 0.117$ [5]. For the strange quark mass parameter we then obtain

$$m_s = 298^{+47}_{-23} \text{ MeV} \quad (11)$$

using the scale-independent relation Eq. (9). This value of m_s is not significantly different from the previous determination and we shall use it in our fragmentation functions Eqs. (5) – (6). The strong coupling constant in Eqs. (5) – (6) then has the value $\alpha_s(2m_s) = 0.745$. While this value of α_s is uncomfortably large we note that it only enters, together with m_s and $R(0)$, in the normalization of the fragmentation functions, which has been determined empirically through Eq. (9).

V. RESULTS AND DISCUSSIONS

The evolution equations were numerically integrated and the fragmentation functions at the scale $\mu_R = \sqrt{p_T^2(\text{parton}) + m_b^2}$ were combined with the structure functions and parton cross sections for the subprocesses to obtain the cross section, Eq. (1). Specifically, we calculated the transverse momentum distributions of B_s and B_s^* mesons produced in $p\bar{p}$ collisions at the Tevatron energy $\sqrt{s} = 1.8$ TeV. We assumed a cut-off on the transverse momentum of $p_T > 5$ GeV/ c^2 and considered only the rapidity range $|y| < 1$. In Fig. 1 we show the cross section $d\sigma/dp_T$ for both B_s and B_s^* . To investigate the sensitivity of these results to the scale μ we have also included the results for $\mu = 2\mu_R$ and $\mu = \mu_R/2$. When the scale μ is less than $\mu_0 = m_b + 2m_s$, which only happens for the case of $\mu = \mu_R/2$, we chose the larger of (μ, μ_0) . From Fig. 1 it is clear that the choice of scale μ is not critical for the transverse momentum distribution; in fact, the variation over the range $\mu_R/2 < \mu < 2\mu_R$ is comparable to the current discrepancies between the measured and calculated b production cross sections. As one might expect, the (3S_1) B_s^* cross section is larger than the (1S_0) B_s cross section at all p_T , however, their ratio is not precisely the naive prediction 3 : 1, but is about 20% smaller.

In Fig. 2 we show the total cross section for the production of B_s and B_s^* mesons with transverse momentum above a minimum value p_T^{\min} . As in Fig. 1 only the range $p_T > 5$ GeV and $|y| < 1$ was considered. The sensitivity to the scale μ was investigated, as before, by considering $\mu = \mu_R/2$ and $\mu = 2\mu_R$, and the choice of this scale is clearly not critical. Figure 2 provides useful estimates of the production rates of B_s and B_s^* mesons at the Tevatron due to the fragmentation process. For convenience, we have also presented these cross section estimates in Table I, including the sum $\sigma(B_s) + \sigma(B_s^*)$.

The production rates and transverse momentum distributions for B_s and B_s^* meson production in $p\bar{p}$ collisions presented here assume that fragmentation is the dominant process and, therefore, are probably underestimates. At large enough transverse momentum the fragmentation process should dominate, as it falls off more slowly, even though it is only a part of the full order α_s^4 contribution. We also note that in our calculation the light quark fragmentation contribution is not included, since it is of even higher order in α_s than the induced gluon fragmentation. At the initial heavy quark mass scale, the light quark fragmentation function $D_{q \rightarrow B_s}(z, \mu)$ is of order $\alpha_s^4 (\alpha_s^2)$ for $q = u, d (q = s)$. But the $D_{s \rightarrow B_s}(z, \mu)$ has been shown [7] to be suppressed by $(m_s/m_b)^3$ relative to $D_{\bar{b} \rightarrow B_s}(z, \mu)$. Therefore, at the initial scale none of these light quark fragmentation functions are important. The light quark fragmentation functions might acquire a logarithmic enhancement from the evolution of the Altarelli-Parisi equations, but the splitting kernels $P_{g \rightarrow q}(x, \mu)$ and $P_{q \rightarrow g}(x, \mu)$ are of order α_s , while $P_{b \rightarrow q}(x, \mu)$ and $P_{q \rightarrow b}(x, \mu)$ are of order α_s^2 . Therefore, the most important sources of induced light quark fragmentation come from (i) $P_{q \rightarrow \bar{b}} \otimes D_{\bar{b} \rightarrow B_s}(z)$, and (ii) $P_{q \rightarrow g} \otimes D_{g \rightarrow B_s}(z)$. Hence, the order of the induced light-quark fragmentation functions at the scale μ can be at most of order $\alpha_s^4 \times \log(\mu/m_b)$, which is suppressed by α_s relative to the induced gluon fragmentation. Since the induced gluon fragmentation only contributes at about the 15–20% level, which is mostly due to the large gluon luminosity at low x , the induced light-quark fragmentation contribution is expected to be very small, at the level of a few %. And thus, the light quark contribution can be safely ignored in compare with other uncertainties in the calculation.

Our fragmentation functions, which we used for the boundary conditions for the Altarelli-Parisi equations at the scale of the heavy b quark mass, are rigorously correct in perturbative QCD if the constituent quarks are much heavier than Λ_{QCD} ; e.g, B_c mesons. Also higher order QCD corrections can, in principle, be systematically calculated. In the case of the B_s meson, higher order corrections in the fragmentation functions might be large due to the fact that the strong coupling constant is evaluated at $2m_s$ and is equal to about 0.75. But we fitted the parameter m_s to the experimental measurement of the total probability for $\bar{b} \rightarrow B_s + B_s^*$ and m_s turned out to be about 300 MeV/ c^2 . We can, therefore, be confident of the overall normalization, which is proportional to $\alpha_s^2(2m_s)|R(0)|^2/m_s^3$. The shapes of the fragmentation functions are only moderately sensitive to the value of m_s and comparing our results for the momentum distribution will, therefore, primarily test the assumption that their *shapes* are adequately given by perturbative QCD at the scale of the b quark mass.

Our approach also appears somewhat similar to the approach used in some Monte Carlo programs, e.g., PYTHIA [12] and HERWIG [13]. However, the main difference lies in the fragmentation of the partons. The fragmentation models used in PYTHIA or HERWIG are rather different in spirit from our perturbative QCD fragmentation, and is based on string fragmentation, though the actual fragmentation models used in these two Monte Carlo programs are somewhat different from each other. In the string fragmentation picture, given an initial q_0 , it is assumed that a new $q_1\bar{q}_1$ pair may be created according to some pre-assigned probabilities such that a meson $q_0\bar{q}_1$ is formed and a q_1 is left behind. This q_1 may at a later stage pair off with a \bar{q}_2 , and so on. The relative probabilities used in PYTHIA to create $u\bar{u}$, $d\bar{d}$, $s\bar{s}$, $c\bar{c}$ pairs are set at $1 : 1 : \gamma_s : \gamma_c$, where $\gamma_s = 0.3, \gamma_c = 10^{-11}$ are default values. This choice is based on a quantum mechanical effect and is only approximate. For example, in a paper by Lusignoli et al. [14], in order to reproduce the B_c meson production using HERWIG to within a reasonable range, they had to increase the probabilities of creating $c\bar{c}$ pairs in the cluster splitting. Thus, this ad hoc feature of string fragmentation in these Monte Carlo programs makes it less predictive than our perturbative QCD fragmentation functions, because in our perturbative QCD fragmentation model the probability for $\bar{b} \rightarrow B_s, B_s^*$ is

determined reliably once m_b , m_s , as well as the nonperturbative parameter of the bound-state, e.g., the decay constant f_{B_s} , are given. The string fragmentation picture is rather phenomenological since the parameter γ_s can be adjusted freely to fit the experimental measurements. Another weakness of such a string fragmentation model is that it must assume the B_s/B_s^* ratio of 1/3, from naive spin counting, while our perturbative QCD fragmentation model can reliably predict this ratio once m_s is given. In fact, the ratio is slightly larger (20%) than 1/3, as expected for a non-zero m_s , in the HQET [15] in which m_s/m_b is the leading heavy quark-spin symmetry breaking effect.

The comparison with forthcoming data from the Fermilab Tevatron should be instructive.

This work was supported by the U. S. Department of Energy, Division of High Energy Physics, under Grant DE-FG02-91-ER40684 and DE-FG03-93ER40757.

REFERENCES

- [1] P. Abrau *et al.* (DELPHI Collaboration), *Z. Phys* **C61**, 407 (1994).
- [2] K. Cheung and R.J. Oakes, *Phys. Lett.* **B337**, 181 (1994).
- [3] K. Cheung, *Phys. Rev. Lett.* **71**, 3413,(1993); K. Cheung and T.C. Yuan, *Phys. Lett.* **B325**, 481 (1994); K. Cheung and T.C. Yuan, preprint CPP-94-37 (Feb 1995), hep-ph/9502250.
- [4] H.L. Lai *et al.* (CTEQ Collaboration), *Phys. Rev.* **D51**, 4763 (1995).
- [5] Particle Data Group, *Phys. Rev.* **D45**, 51 (1992).
- [6] G. Altarelli and G. Parisi, *Nucl. Phys.* **B126**, 298 (1977).
- [7] E. Braaten, K. Cheung, and T. C. Yuan, *Phys. Rev.* **D48**, R5049 (1993).
- [8] R. Van Royen and V. Weisskopf, *Nuovo Cimento* **50**, 617 (1967); **51**, 583 (1967).
- [9] C. Bernard, J. Labrenz, and A. Soni, *Phys. Rev.* **D49**, 2536 (1994).
- [10] DELPHI Coll., *Phys. Lett.* **B289**, 199 (1992); ALEPH Coll., *Phys. Lett* **B294**, 145 (1992); OPAL Coll., *Phys. Lett.* **B295**, 357 (1992).
- [11] T.J. LeCompte (CDF Collaboration), submitted paper to the 27th Int. Conf. on High Energy Physics, Glasgow, Scotland, 20–27 July 1994, FERMILAB-CONF-94/134-E.
- [12] *PYTHIA 5.7 and JETSET 7.4: Physics and Manual*, T. Sjostrand, hep-ph/9508391; *Comput. Phys. Commun.* **82**, 74 (1994).
- [13] G. Marchesini *et al.*, *Comput. Phys. Commun.* **67**, 465 (1992).
- [14] M. Lusignoli, M. Masetti, and S. Petrarca, *Phys. Lett.* **B266**, 142 (1991).
- [15] E. Braaten, K. Cheung, S. Fleming, and T.C. Yuan, *Phys. Rev.* **D51**, 4819 (1995).

TABLES

TABLE I. Total B_s and B_s^* cross sections in nb versus p_T^{\min} for $p_T > 5$ GeV and $|y| < 1$ at $\sqrt{s} = 1.8$ TeV. Variation with the scale μ are shown.

p_T^{\min}	$\sigma(B_s)$			$\sigma(B_s^*)$			$\sigma(B_s) + \sigma(B_s^*)$		
	$\underline{\mu_R/2}$	$\underline{\mu_R}$	$\underline{2\mu_R}$	$\underline{\mu_R/2}$	$\underline{\mu_R}$	$\underline{2\mu_R}$	$\underline{\mu_R/2}$	$\underline{\mu_R}$	$\underline{2\mu_R}$
5	300	470	650	700	1100	1500	1000	1600	2200
10	45	62	65	110	145	150	150	210	220
15	14	16	14	32	37	33	46	52	47
20	5.2	5.1	4.4	12	12	10	17.5	17	15

FIGURE CAPTIONS

1. The transverse momentum distributions of B_s and B_s^* mesons for $p_T > 5$ GeV, $|y| < 1$, and $\mu = \mu_R/2, \mu_R$, and $2\mu_R$ at $\sqrt{s} = 1.8$ TeV.
2. The B_s and B_s^* total cross sections for $p_T > p_T^{\min}$ with $p_T > 5$ GeV, $|y| < 1$, and $\mu = \mu_R/2, \mu_R$, and $2\mu_R$ at $\sqrt{s} = 1.8$ TeV.

FIGURES

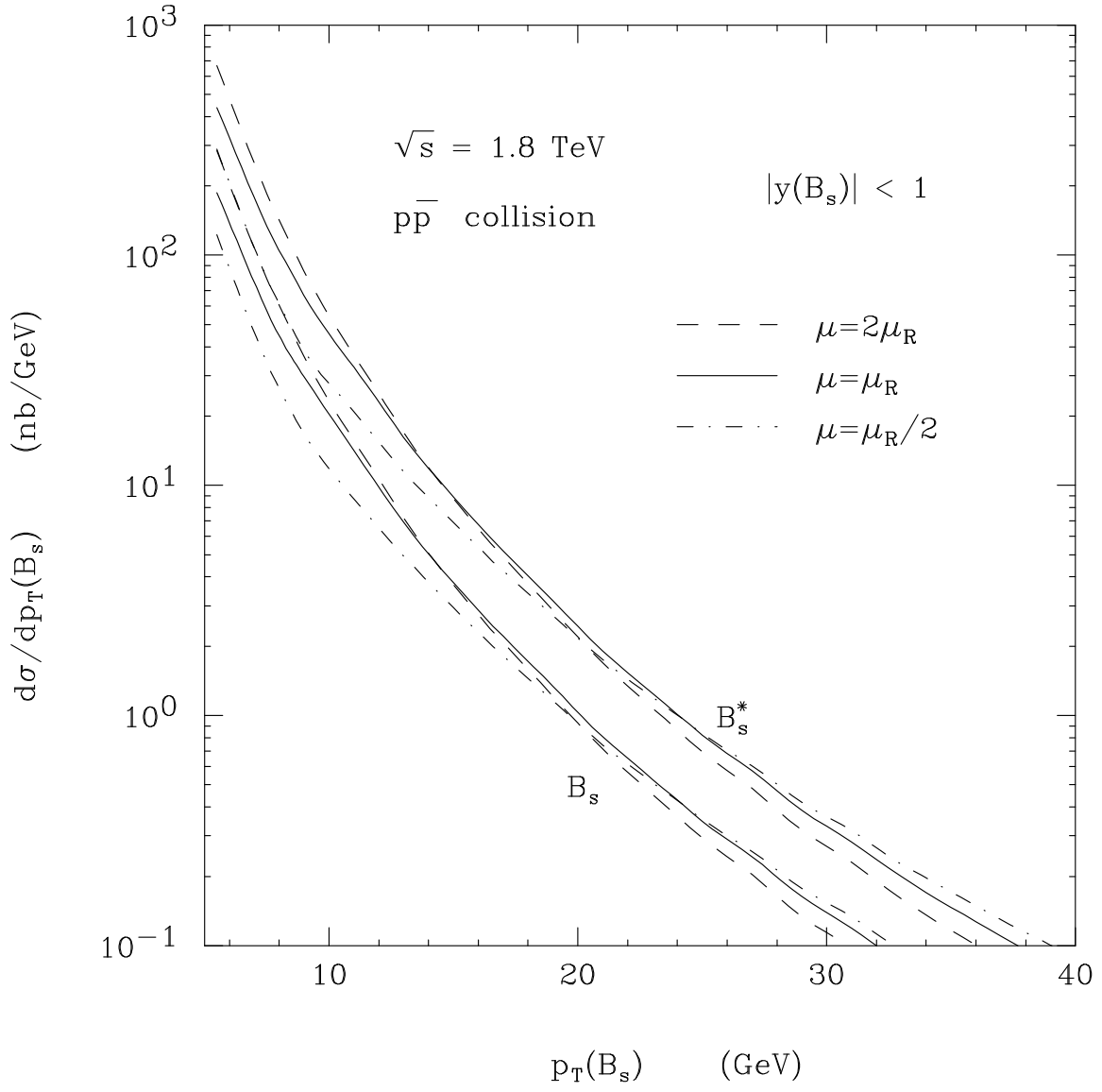


FIG. 1.

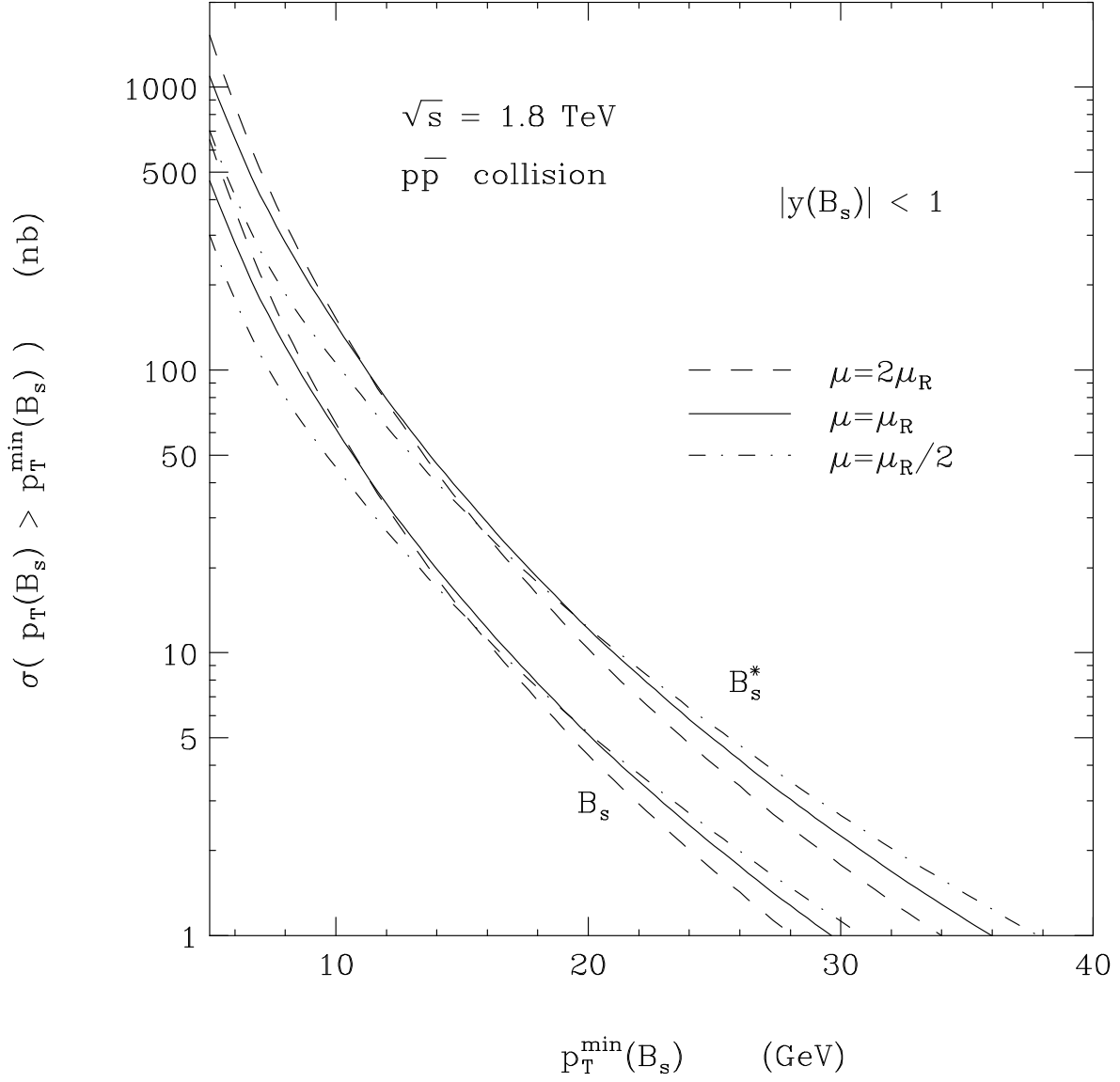


FIG. 2.